JOURNAL OF MATERIALS SCIENCE 23 (1988) 2069–2075

Phase stability of B1-type carbides in nickel-based alloys

YOSHINORI MURATA, RYUZI NINOMIYA*, NATSUO YUKAWA
*Department of Production Systems Engineering, and *Graduate School, Toyohashi University of Technology, Hibarigaoka, Tempaku-cho, Toyohashi 440, Japan*

In nickel-based superalloys, the B1-type monocarbides contain several kinds of transition elements. At elevated temperatures, the monocarbides transform to other carbides, such as $M_{23}C_6$ and M_6C as a result of the reaction with the alloy. The phase stability of monocarbides was investigated by X-ray diffraction techniques. The degree of stability is strongly affected by the composition of the monocarbides and is related generally to the magnitude of the lattice parameter of the monocarbides. That is, the larger the lattice parameters of the monocarbides, the higher their stability in nickel-based alloys.

1. Introduction

Transition metals of the subgroups IVa, Va and VIa form cubic monocarbides with carbon, that have the sodium chloride-type structure. The carbide is formed during solidification from the melt in most nickel-based superalloys. The carbide contains several kinds of transition metals which are components of the superalloys [1–5]. In general, the monocarbide in nickel-based superalloys is known to transform to other carbides such as $M_{23}C_6$ and M_6C, etc., during exposure at elevated temperatures as a result of the reaction between the carbon atoms in the monocarbide and the elements in the matrix of superalloys. According to the results of Collins' report [6], the qualitative phase stability of the monocarbides in a series of superalloys is different from alloy to alloy. Therefore, it is considered that the phase stability is dependent on the chemical composition of monocarbides, but the relationship between the stability and the chemical composition has been open to debate.

Recently, we investigated the effect of transition elements on the composition of the monocarbide in one of the superalloys, IN-100, and obtained the following results: (1) the monocarbide in IN-100 was the titanium-rich one, and the composition was affected severely by the doping of 0.81 at.% niobium, tantalum or tungsten; (2) when IN-100 was doped with zirconium, the zirconium-rich monocarbide in addition to the titanium-rich one was formed; (3) when IN-100 was doped with hafnium, the hafnium-rich monocarbide was formed in addition to the titanium-rich monocarbide. From these results we also suggested that the chemical composition of the carbide in the alloy was determined by two factors, one of which was the radius of metal atoms in each monocarbide, and the other the standard free energy of formation of each monocarbide [5]. Using our systematic data on the chemical composition of the monocarbides, we can study the effect of composition on the phase stability. In this paper, we report an investigation of the phase stability of the monocarbide on the basis of a model experiment, and propose a factor to evaluate the phase stability.

Transition metal monocarbides have great hardness, high melting point, thermal and electrical conductivity, etc. Therefore, they are candidates for use as the coating material of the first wall of a fusion reactor [7], and for an electron gun [8, 9]. They have also been used as the main component for hard materials, in which cobalt-based alloys or nickel-based alloys are used as a binder metal. In these fields, the reaction between the monocarbide and alloys will be important. For example, in hard materials, the phase stability of the monocarbide is related to the properties such as wear resistance [10]. Therefore, data and an understanding of the phase stability of monocarbides are important for its practical application.

2. Experimental procedure

To investigate the phase stability of monocarbides in superalloys, we employed IN-100, the doped alloys (which are prepared by the doping of IN-100 with transition elements) and model alloys.

2.1. Carbides in IN-100 and doped alloys

The composition of IN-100 is shown in Table I. In the as-cast state, only NaCl-type monocarbide was observed in IN-100, and the composition was TiC and $(Ti_{0.80}Mo_{0.17}V_{0.03})C$ [5]. In this study, the niobium-, tantalum- and tungsten-doped IN-100 were also prepared because the elements used as the dopants greatly change the composition of the monocarbide in IN-100. The compositions of monocarbides in each doped alloy were reported in the previous paper [5], and the results are shown in Table II.

The dopant and IN-100 were melted together in an arc-furnace under a purified argon atmosphere to produce a button ingot of each doped alloy. The button ingots, each weighing ~ 0.01 kg, were annealed at 1255 K for various periods, and then the carbides were extracted electrolytically from the ingots using a methanol solution with 10% hydrochloric acid and

0022–2461/88 $03.00 + .12

TABLE I Chemical composition (at.%) of IN-100 used

Cr	Co	Mo	Ti	Al	V	C	B	Zr	Ni
9.23	12.63	1.67	3.40	11.09	0.81	0.72	0.075	0.022	bal.

N, 23 at. p.p.m.; O, 30 at. p.p.m.

1% tartaric acid as electrolyte. Because the size of each extracted carbide is less than several tens of micrometres, the carbides were like powder. The extracted carbide powder and an α-titanium powder which was selected as a standard material, were mixed together in the same proportions by weight. Using the mixed powder, the ratio of the monocarbide to the extracted carbides was analysed by an internal standard method of X-ray analysis [11] using Cu$K\alpha$ radiation and a step scan of 1/20 deg at an interval of 10 sec. The 1 1 1 reflection of the monocarbide, 5 1 1 and 3 3 3 reflections of $M_{23}C_6$ carbide, and $0 1 \bar{1} 1$ reflection of α-titanium were used in the analysis.

In the internal standard method, the weight fraction of the phase, W, and the integrated intensity, I, have the following relationship,

$$\frac{I^{(hkl)}_{\text{Phase}}}{I^{(h'k'l')}_{\text{Standard}}} = K\frac{W^{(hkl)}_{\text{Phase}}}{W^{(h'k'l')}_{\text{Standard}}},$$

where K is a constant for the particular set of diffracting planes.

The values of K were determined by the following procedure. Firstly, several kinds of monocarbides, as shown in Table III, were melted by a method which will be mentioned in Section 2.3. The composition of the melted monocarbides (Table III) corresponds to the composition of the monocarbides in the doped alloys (see Table II). Secondly, these carbides were crushed and the $Cr_{23}C_6$ powder was mixed in several different proportions. Thirdly, these mixed carbides and the titanium powder were mixed in the same proportion by weight. Because the weight fractions of the monocarbide and $M_{23}C_6$ carbide are known in these samples, K is determined by the integrated intensity of the 1 1 1 reflection of the monocarbide, 5 1 1 and 3 3 3 reflections of $M_{23}C_6$ carbide, and the $0 1 \bar{1} 1$ reflection of titanium.

2.2. TEM observation of the monocarbide in IN-100

Transmission electron microscopic observations of IN-100 cooled from a melt at a rate of $0.083\,\mathrm{K\,sec^{-1}}$ ($5\,\mathrm{K\,min^{-1}}$) were carried out, in order to examine the orientation relationships between the monocarbide and the alloy matrix. The foils suitable for the observation were prepared by jet dimpling a 3 mm disc with a 75% aqueous hydrochloric acid solution at 50 V, followed by electrolytic polishing in a 20% nitric acid–80% methanol solution at 220 K.

TABLE II Chemical composition of the monocarbides in IN-100 and the doped alloys

IN-100	$(Ti_{0.80}Mo_{0.17}V_{0.03})C$
+ Nb	$(Ti_{0.60}Nb_{0.30}Mo_{0.10})C$
+ Ta	$(Ti_{0.66}Ta_{0.27}Mo_{0.07})C$
+ W	$(Ti_{0.76}Mo_{0.11}W_{0.10}V_{0.03})C$

Carbon content was calculated based on 50 carbon atoms for every 50 metal atoms [5].

TABLE III Nominal composition of the monocarbides prepared for X-ray experiments

IN-100	$(Ti_{0.80}Mo_{0.20})C$
+ Nb	$(Ti_{0.60}Nb_{0.30}Mo_{0.10})C$
+ Ta	$(Ti_{0.66}Ta_{0.27}Mo_{0.07})C$
+ W	$(Ti_{0.77}Mo_{0.13}W_{0.10})C$

2.3. Model experiment

A model experiment was attempted to investigate the phase stability of the monocarbides in superalloys. For this experiment, model monocarbides containing niobium and titanium, and model alloys were newly prepared. Their chemical compositions are shown in Table IV. The powder of niobium monocarbide and titanium monocarbide produced by High-Purity Chemical Co. (Saitana, Japan) was melted by a tri-arc furnace using optical-grade graphite electrodes and a graphite hearth on a water-cooled copper hearth, and model monocarbides were made. The model monocarbides prepared were all identified as single-phase monocarbides by conventional X-ray diffraction. In these monocarbides, the carbon content (x of MC_x) ranged between 0.93 and 0.95. Therefore, the fluctuation of carbon content is negligible for the experimental results in this research. We will abbreviate MC_x to MC such as TiC and (Ti,Nb)C, hereafter. In order to obtain the ingots of model alloys, 99.99% nickel, 99.99% aluminium, 99.95% chromium and 99.99% titanium were melted by an induction furnace under a purified argon atmosphere, and then sucked up by a silica tube.

A model monocarbide-chip, about 0.0001 kg in weight, and a piece of the model alloy, about 0.01 kg in weight, were cut mechanically from the prepared model monocarbide and ingot, respectively. The cut piece of the alloy was melted in the tri-arc furnace using tungsten electrodes and a water-cooled copper hearth. The carbide chip was inserted into the melt of the alloy, and immediately the power of the arc furnace was turned off, to give the button ingots including a carbide chip approximately at the centre. On turning off the power, the samples were cooled quickly by the water-cooled copper hearth; therefore, during the cooling, the reaction between the monocarbide and the alloy appears to be negligible.

The button ingots were annealed at 1255 K for various periods to transform the monocarbide into $Cr_{23}C_6$ carbide, and then all carbides in the button ingots were extracted electrolytically using a similar electrolyte to that mentioned in Section 2.1. The ratio

TABLE IV The nominal composition of monocarbides and alloys prepared for a model experiment

Monocarbides	Alloys (at.%)
TiC	
$(Nb_{0.75}Ti_{0.25})C$	Ni-10Cr-10Al-5Ti
$(Nb_{0.50}Ti_{0.50})C$	
$(Nb_{0.25}Ti_{0.75})C$	Ni-10Cr-15Al
NbC	

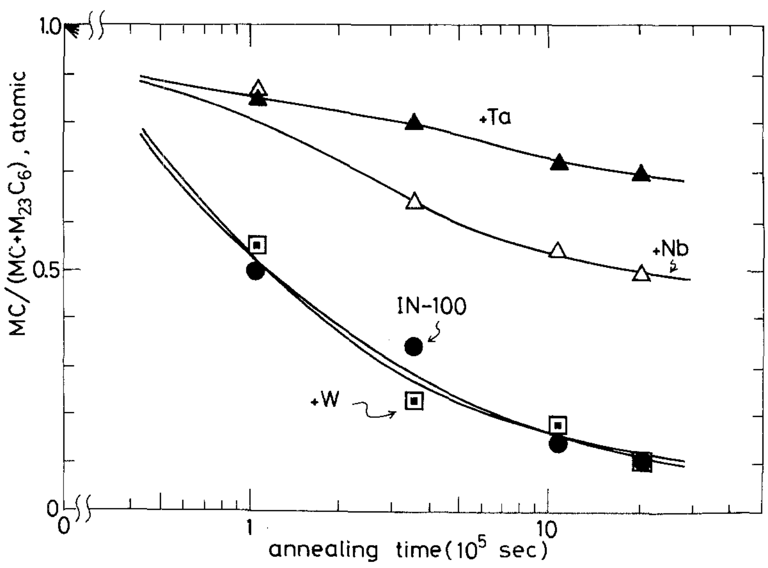

Figure 1 Change in the amount of monocarbides in IN-100 and the doped alloys with annealing at 1255 K.

of the monocarbide to all carbides was analysed quantitatively by the internal standard methods, as mentioned in Section 2.1. Also, the interface between the monocarbide and the alloy of the button ingots was observed using a secondary electron microscope (Hitachi X-650).

3. Results

3.1. Phase stability of the monocarbides in IN-100 and the doped alloys

It is known that only the $M_{23}C_6$ carbide is formed by the transformation of the monocarbide during annealing at elevated temperatures in IN-100 [6], and also, that in the niobium-, tantalum- and tungsten-doped alloys, a similar carbide reaction is observed after annealing at 1255 K. Therefore, only two kinds of carbides, the monocarbide and $M_{23}C_6$ carbide, were observed in the X-ray diffraction of the carbides extracted from IN-100 and the annealed doped alloys. Fig. 1 shows the change in the amount of monocarbide, which was extracted electrolytically from the alloys after annealing for varied periods of time. The ordinate represents the atomic ratio of the monocarbide to the total carbides extracted. The (Ti,Mo,V)C carbides in IN-100, and the (Ti,Mo,W)C carbide in the tungsten-doped alloy (see Table II) transformed quickly to $M_{23}C_6$ carbide, and after 3.6×10^5 sec annealing, the atomic fraction of the $M_{23}C_6$ carbide came to almost 0.7, as can be seen in the figure. On the other hand, the monocarbide in the niobium-doped alloy changed slowly into $M_{23}C_6$ carbide, and the slowest changing rate was observed in the tantalum-doped alloy.

As is shown in Table II, the monocarbides in the tantalum- and niobium-doped alloys contain about 30% tantalum and niobium, respectively, and these monocarbides are stable compared with the monocarbide in IN-100 (Fig. 1). This fact indicates that the chemical composition of the monocarbide severely affects its stability. In the tungsten-doped alloys, the stability of the monocarbide is unchanged compared with that in IN-100. It is consistent with the results of the previous report [5] that tungsten is quite similar to molybdenum in character.

3.2. Model experiment

As mentioned above, the monocarbides containing niobium and tantalum were more stable than the titanium-rich monocarbide. Also, the zirconium-rich monocarbide was reported to be very stable compared with the titanium-rich monocarbide [12], in spite of the fact that zirconium belongs to the same group in the periodic table as titanium. In view of these results, we attempted, with the model experiment (see Section 2.3), to reveal the factor which determines the phase stability of the monocarbides in nickel-based alloys.

Fig. 2 represents the interface between the model alloy and the model monocarbide in a model specimen

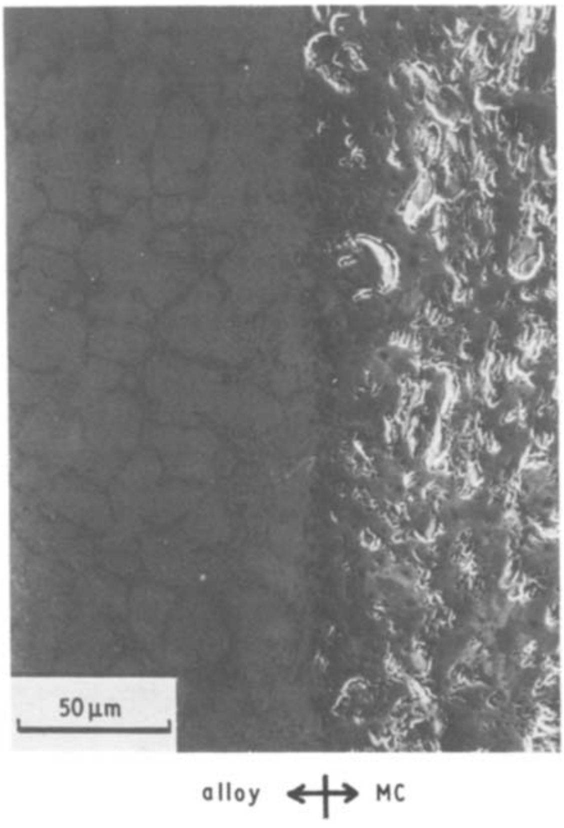

Figure 2 Scanning electron micrograph, showing a representative interface between the alloy and monocarbide in the model specimen.

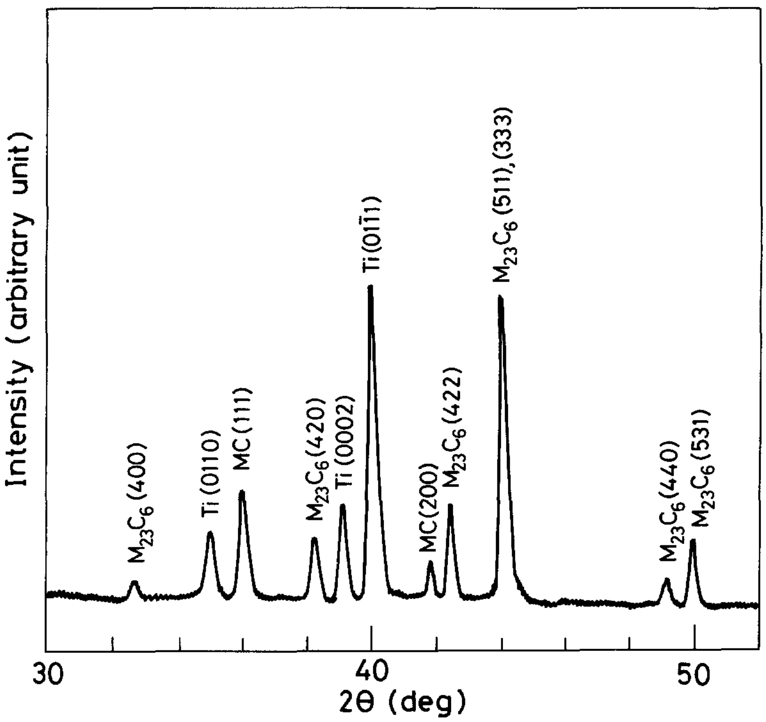

Figure 3 A representative results of X-ray diffraction of residual carbides extracted from one of the model specimens. Cu*Kα* radiation.

which is in a prepared state. The contact at the interface was perfect. During annealing, the model monocarbide transformed to other carbides as a result of the reaction with the alloy. Fig. 3 is a representative result of X-ray diffraction of the extracted carbides from one of the model specimens, $(Nb_{0.25}Ti_{0.75})C$, after annealing at 1255 K for 3.6×10^5 sec. As can be seen in the figure, only the monocarbide and $M_{23}C_6$ carbide were observed. The product carbide of the transformation was the $M_{23}C_6$ carbide in all model specimens. The amounts of the monocarbide and the newly formed $M_{23}C_6$ carbide extracted from the model specimen were analysed by the internal standard method of X-ray diffraction. The results are shown in Fig. 4. Square symbols represent the results obtained from the model specimens which consist of the (Nb,Ti)C model carbide and the Ni–Al–Cr–Ti quaternary alloy. Circles represent the results of the specimens which consist of the (Nb,Ti)C and the Ni–Al–Cr ternary alloy. The atomic fraction of the monocarbide is represented on the left-hand ordinate of the figure. For reference, the ratio of the amount of consumed carbon in $M_{23}C_6$ carbide to that of carbon in the model monocarbide is given on the right-hand ordinate. The amount of the monocarbide decreased with increasing TiC fraction in the model monocarbide. Although this tendency was similar in both quaternary and ternary alloys, it was found that the volume fraction of $M_{23}C_6$ carbide formed in the quaternary alloy was greater than in the ternary one, regardless of the composition of the monocarbides.

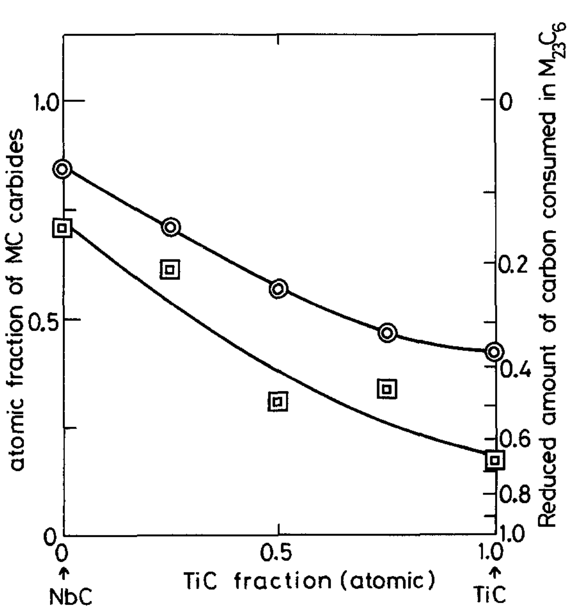

Figure 4 The dependence of TiC fraction in the model monocarbides upon the fraction of monocarbide in the total amount of carbides in the model specimens after annealing at 1255 K for 3.6×10^5 sec: (▣) in Ni-Al-Cr-Ti, (◎) in Ni-Al-Cr.

Fig. 5 shows typical photographs of the model specimen after annealing, and a schematic illustration of the carbide phases in the button ingot. The photographs are taken from the two circled areas in the illustration, one of which is at the interface and the other in the alloy matrix. On the matrix alloy side of the interface, which is seen like a crevice in the photograph, the monocarbide phase, which is shown in the grey phase, was formed. The crevice was the metal–monocarbide interface before annealing. The results of X-ray line analysis using Nb*L* shows that the intensity level of the niobium spectrum was almost the same on both sides of the crevice. Therefore, the monocarbide formed newly in the matrix side was considered to have a similar composition to the model monocarbide. On the other hand, a fine $M_{23}C_6$ carbide was observed in the matrix far away from the interface as well as near to the interface. This carbide is shown in a series of photographs on the right-hand side of Fig. 5. The size of the $M_{23}C_6$ carbide was 2 to 3 μm, and it was almost $Cr_{23}C_6$ carbide. These characteristics of the morphology of the annealed specimens were similar in all model specimens.

4. Discussion

The stability of the monocarbides is related to the

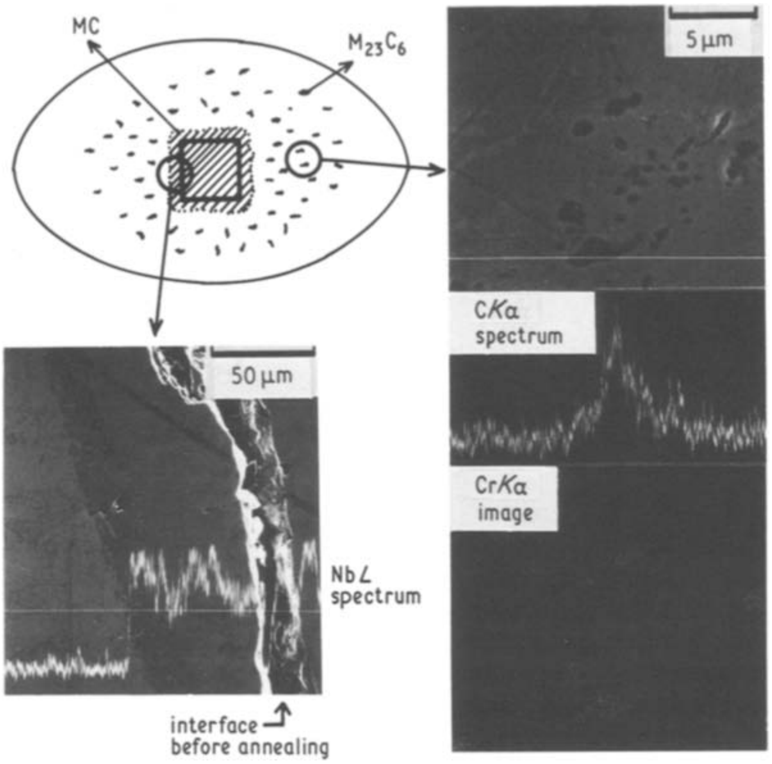

Figure 5 A schematic illustration and typical photographs of the carbide phases in the model specimen after annealing.

activity of carbon and transition metal atoms in the nickel-based alloys. However, the chemical compositions of the monocarbides change with the composition of the alloys, and furthermore, the alloy usually contains more than ten elements. Therefore, it is difficult to determine the activity, even though it is very important.

Generally, transition-metal monocarbides are considered to be very stable compared with $M_{23}C_6$ carbides in view of the standard Gibbs free energy of formation [13, 14], but the monocarbides in nickel-based alloys transform to $M_{23}C_6$ carbide during exposure at elevated temperatures [15]. The rate of this transformation depended on the chemical composition of the monocarbides (see Fig. 1). The difference in the transformation rate has not been explained even qualitatively with respect to the melting points and averaged valence values of the monocarbides. For example, it is reported that a zirconium-rich monocarbide did not transform in the IN-100 type alloy during annealing up to at least 1.8×10^6 sec [12], in spite of the fact that the melting temperature of zirconium monocarbide is lower than those of hafnium and niobium monocarbides. On the other hand, zirconium and titanium monocarbides have the same averaged valence values, but the stability of the two monocarbides is quite different.

$M_{23}C_6$ carbide which is formed by the transformation of the monocarbides is reported to appear mainly in the $\{1\,1\,1\}$ planes of the matrix [2]. In the nickel-base superalloys, $M_{23}C_6$ carbide is almost a $Cr_{23}C_6$ carbide. In the matrix of the nickel-base alloys, the arrangement of atoms in the $\{1\,1\,1\}$ plane take the shape of triangles, and the distance between atoms is about 0.25 nm. Although $Cr_{23}C_6$ has a complex structure, the distance between the metal atoms in the $\{1\,1\,1\}$ plane is 0.25 nm which is calculated using the lattice parameter, 1.066 nm [16]. These facts imply that there is only a small misfit between the $M_{23}C_6$ carbide and the nickel-based alloy. Considering these results, the coherency strain between nickel-based alloy and monocarbides plays an important role in the phase stability of the monocarbides. Therefore, it is significant to consider the relationship between the phase stability and the lattice parameters of the monocarbides, because the latter is an indication of the coherency strain in the superalloys. Fig. 6 shows the stability plotted against the lattice parameter of the monocarbides. The figure contains all the data obtained from the experiment using the doped alloys, the ternary alloy, and the quaternary alloy. The ordinate in Fig. 6 is the same as those in Figs 1 and 4, and represents the stability of the monocarbide after annealing for 3.6×10^5 sec. The value of 1.0

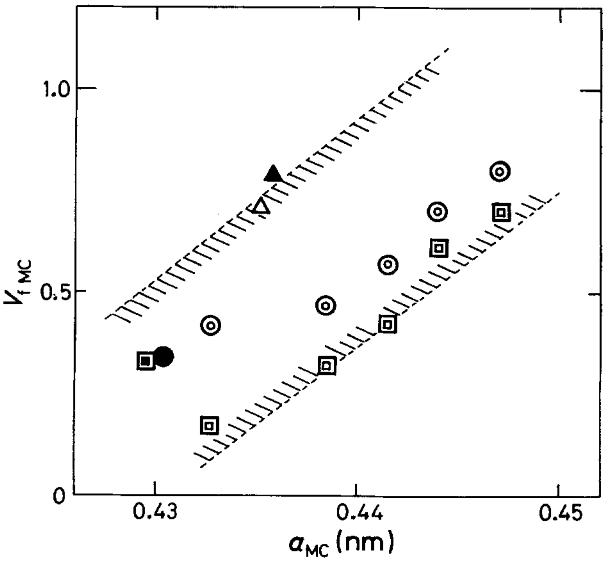

Figure 6 The relationship between lattice parameter of the monocarbides, a_{MC}, and the fraction of the monocarbide in the total amount of carbides, V_{fMC}, in nickel-based alloys after annealing at 1255 K for 3.6×10^5 sec.

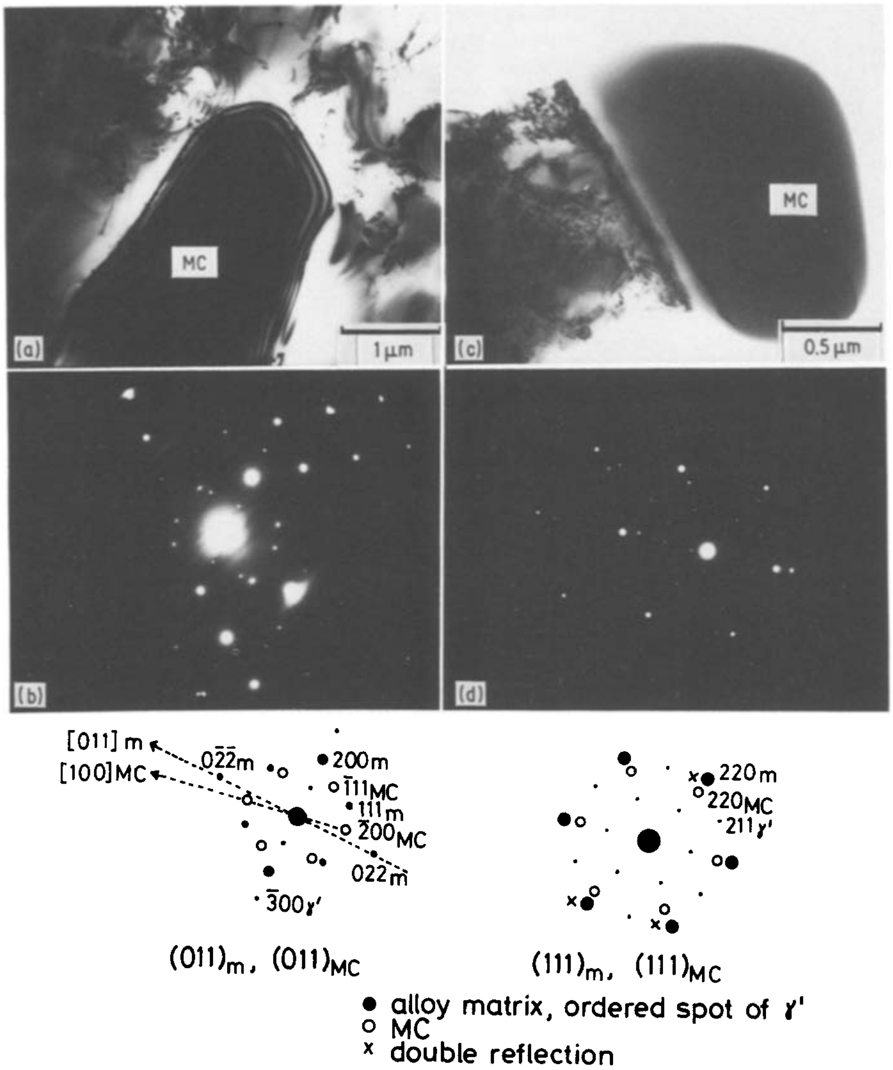

Figure 7 Transmission electron micrographs showing the interface between the monocarbide and the alloy matrix in IN-100.

corresponds to the result when the monocarbide did not transform after annealing. As can be seen in the figure, the larger the lattice parameter of the monocarbides, the higher the stability. The tendency was independent of the type of matrix alloy. The result represented in Fig. 6 will be applicable in cases when stability of monocarbides is necessary in the nickel-based alloys and in the interface between nickel-based alloys and the monocarbides.

Fig. 7 shows transmission electron micrographs of the interface between the monocarbide and alloy matrix in IN-100. Figs 7b and d, which are the diffraction patterns of (a) and (c) respectively, are obtained from both phases of the monocarbide and matrix. Piearcey and Smashey [2] reported that no orientation relationship existed between the primary monocarbides and the matrix in Mar-M 200 alloy [2]. However, most monocarbides in IN-100 had orientation relationships, which were almost $[1\,1\,0]_{\text{matrix}} \parallel [1\,0\,0]_{\text{MC}}$ or $[1\,0\,0]_{\text{matrix}} \parallel [1\,0\,0]_{\text{MC}}$, as indicated in (b) and (d). These orientation relationships indicate that coherency between the monocarbide and alloy matrix existed when the size of the monocarbide was very small at the initial stage of formation, but when the size of the monocarbide was large, it was impossible to maintain the coherency because of the large difference between the lattice parameters of the two phases. A number of dislocations found in the alloy matrix (in (a) and (c)) indicate that a large strain is stored in the matrix even after the breaking out of the coherency. On the basis of the two orientation relationships, the arrangement of atoms in the monocarbides and that of atoms in the matrix can be considered to be as shown in Fig. 8. In both cases, if the lattice parameter of the monocarbide were to become large, the mismatch between the two phases might become small. The assumption is consistent with the result that the larger the lattice constants, the higher the phase stability of the monocarbides (Fig. 6).

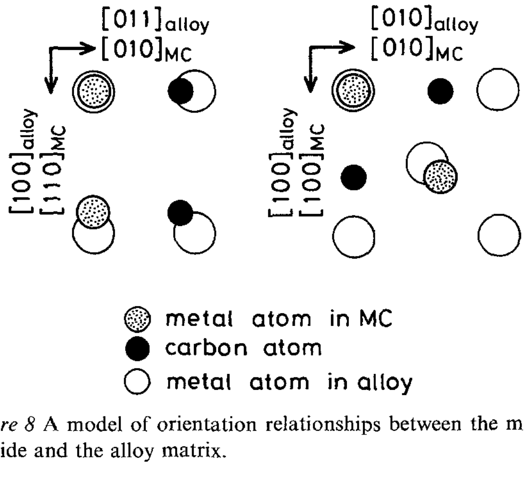

Figure 8 A model of orientation relationships between the monocarbide and the alloy matrix.

5. Conclusion

The stability of transition metal monocarbides, which have several kinds of transition metals for each monocarbide in nickel-based alloys, was investigated by X-ray diffraction using the internal standard method.

From the experimental results, it was concluded that the lattice parameter of monocarbides and the stability of the monocarbides in nickel-based alloys are related to each other. That is, the larger the lattice parameter, the higher the stability.

Acknowledgements

The authors wish to thank Professor K. Ito, Associate Professor M. Kawakami and Dr S. Yokoyama of Toyohashi University of Technology for analysing the carbon content of the monocarbides. This work was partly supported by the Ishihara-Asada Research Fund of the Iron and Steel Institute of Japan.

References

1. J. E. RESTALL and E. C. TOULSON, *Metals and Materials* **7** (1973) 134.
2. B. J. PIEARCEY and R. W. SMASHEY, *Trans. AIME* **239** (1967) 451.
3. W. J. BOESH and H. B. CANADA, *J. Metals* **20** (1968) 46.
4. W. V. YOUDELIS and O. KWON, *Metal Sci.* **17** (1983) 385.
5. Y. MURATA, K. SUGA and N. YUKAWA, *J. Mater. Sci.* **21** (1986) 3653.
6. H. E. COLLINS, *Trans. ASM* **62** (1969) 82.
7. T. SHIKAMA, Y. SAKAI, M. FUKUTOMI and M. OKADA, *J. Nuclear Mater.* **133–134** (1985) 765.
8. K. FUJII, S. ZAIMA and Y. SHIBATA, *J. Appl. Phys.* **57** (1985) 1723.
9. K. YADA and H. SHIMOYAMA, *J. Electron Microsc.* **34** (1985) 147.
10. O. KNOTEK and P. LOHAGE, in "Science of Hard Materials", edited by E. A. Almond, C. A. Brookes and R. Warren (Hilger, Bristol, 1986) p. 757.
11. B. D. CULLITY, "Elements of X-ray Diffraction" (Addison Wesley, New York, 1956) p. 408.
12. Y. MURATA and N. YUKAWA, *Scripta Metall.* **20** (1986) 693.
13. R. HULTGREN, P. D. DESAI, D. T. HAWKINS, M. GLEISER and K. K. KELLEY, "Selected Values of the Thermodynamic Properties of Binary alloys" (American Society for Metals, Ohio, 1973).
14. E. K. STORMS, "The Refractory Carbides" (Academic, New York, 1967) pp. 18, 35.
15. A. K. JENA and M. C. CHATURVEDI, *J. Mater. Sci.* **19** (1984) 3121.
16. S. NAGAKURA and S. OKETANI, *Trans. Iron Steel Inst. Jpn* **8** (1968) 265.

Received 27 April
and accepted 6 July 1987